Solar Energy Materials & Solar Cells 111 (2013) 74–81

Contents lists available at SciVerse ScienceDirect

Solar Energy Materials & Solar Cells

journal homepage: www.elsevier.com/locate/solmat

# Optimization of gain and energy conversion efficiency using front-facing photovoltaic cell luminescent solar concentrator design

Carley Corrado [a,1], Shin Woei Leow [a,c,1], Melissa Osborn [a], Emory Chan [b], Benjamin Balaban [a], Sue A. Carter [a,*]

[a] Department of Physics, University of California, Santa Cruz, CA 95064, USA
[b] The Molecular Foundry, Lawrence Berkeley National Laboratory, Berkeley, CA 94720, USA
[c] Jack Baskin School of Engineering, University of California, Santa Cruz, CA 95064, USA

ARTICLE INFO

*Article history:*
Received 9 August 2012
Received in revised form
19 November 2012
Accepted 10 December 2012
Available online 21 January 2013

*Keywords:*
Luminescent solar concentrator
Lumogen Red 305
Building integrated photovoltaic
Front-facing photovoltaic

ABSTRACT

Luminescent solar concentrator (LSC) windows with front-facing photovoltaic (PV) cells were built and their gain and power efficiency were investigated. Conventional LSCs employ a photovoltaic (PV) cell that is placed on the edge of the LSC, facing inward. This paper describes a new design with the PV cells on the front-face allowing them to receive both direct solar irradiation and wave-guided photons emitted from a dye embedded in an acrylic sheet, which is optically coupled to the PV cells. Parameters investigated include the thickness of the waveguide, edge treatment of the window, cell width, and cell placement. The data allowed us to make projections that aided in designing windows for maximized overall efficiency. A gain in power of 2.2 × over the PV cells alone was obtained with PV cell coverage of 5%, and a power conversion efficiency as high as 6.8% was obtained with a PV cell coverage of 31%. Balancing the trade-offs between gain and efficiency, the design with the lowest cost per watt attained a power efficiency of 3.8% and a gain of 1.6 ×.



## 1. Introduction

The worldwide solar energy market has experienced rapid growth in recent years, with installation of new photovoltaic (PV) panels in the US almost doubling year on year. This trend is expected to continue with increasing adoption of solar power, aided by the falling cost of solar generated power [1–2] and rising prices of fossil fuels. Still, depending on regional sunlight condition, solar power is usually not competitive enough compared to fossil fuels. To achieve this requires further reductions in manufacturing and installation cost of solar panels or improvements in PV cell conversion efficiencies.

One approach for lowering the cost of solar power is the use of Luminescent Solar Concentrators (LSCs). LSCs have a dual effect of concentrating light onto a smaller PV area, and downshifting the incoming spectrum to one in which the PV cell has a higher external quantum efficiency [3–14], thereby achieving higher power outputs for the same area of PV cell used. This idea was first proposed in the late 70s [15–18] and has renewed interest due to more stable and efficient luminescent materials available today. With low material and processing cost, the cost per watt of LSC panels can be lower than current PV panels. The ability to concentrate both direct and diffuse light negates the need for expensive solar tracking systems and improves robustness to shading effects. This allows LSC panels to be incorporated into building integrated photovoltaic (BIPV) designs as façade claddings in addition to roof top fixtures. Furthermore, its controllable color and transparency allows the technology to be used in windows, skylights and greenhouse panels. Installation and support structures make up half the cost of current PV panels on the market. BIPV merely adds the cost of the LSC and PV cells to an existing structure thus avoiding the extra installation cost [19–21].

An LSC consists of a flat transparent matrix with luminescent particles, such as organic dyes, quantum dots (QDs), or semiconducting polymers [22–25] dispersed uniformly inside it. Light entering the panel is absorbed by the luminescent particles, which then re-emit the light isotropically. A fraction of the re-emitted light is at an angle smaller than the critical angle and will escape back into air. The remaining undergoes total internal reflection at the LSC/Air interface trapping it in the matrix and guiding it towards the PV cells to be collected, as illustrated by Fig. 1. This effectively concentrates light from a larger surface onto a smaller PV area increasing the power output of the cell. We define a performance parameter, termed gain, which is the increase in output power attributed to the addition of LSC to the

* Corresponding author.
*E-mail address:* sacarter@ucsc.edu (S.A. Carter).
[1] Equally contributing first authors

0927-0248/$ - see front matter © 2013 Elsevier B.V. All rights reserved.
http://dx.doi.org/10.1016/j.solmat.2012.12.030

panel compared to the control cells with equivalent area and PV characteristics, but no luminescent material.

$$\text{Gain} = \text{Power (LSC window)}/\text{Power (control cell)}$$

The most common configuration is to have the PV cell mounted onto the side of the LSC, as in Fig. 1(I). While doing so achieves a high concentration factor, the overall efficiency of the panel is low due to losses from both self-absorption and low solar absorption. Measured panel efficiencies up to 7.1% have been reported with this configuration [4–11]; however, this was obtained using a low concentration factor of 2.5, a diffusive backside reflector, and expensive GaAs PV cells.

In this work, we have adopted a design with the cells mounted front facing, surrounded by luminescent material to absorb both direct sunlight and wave-guided concentrated light, as shown in Fig. 1(II). This layout allows for the PV cells to directly convert the solar irradiance to power, resulting in greater gain [26], and also reduces the distance photons have to travel in the wave-guide. In addition, the LSC was separated into a thin luminescent absorbing layer and a thick waveguide layer, thereby allowing photons to travel a longer distance in the panel without re-absorption [27]. Efficiency of the system can be determined from

$$\eta_{\text{panel}} = (A_{\text{PV}}/A_{\text{panel}})\eta_{\text{PE}} + (A_{\text{LSC}}/A_{\text{panel}})\eta_{\text{PL}} \times \eta_{\text{abs}} \times \eta_{\text{WG}} \times \eta_{\text{DC}} \times \eta_{\text{MPE}}$$

where $A$ is the area and $\eta$ is the efficiency. The subscripts panel, PV, PE, LSC, PL, abs, WG, DC, MPE refer to the overall panel, PV cell, PV conversion efficiency, luminescent material, dye photoluminescence, dye absorption, waveguide, wavelength down-conversion and efficiency at emission wavelength, respectively.

A commercial dye and silicon PV cells were used, thus the values of,$\eta_{\text{PE}}$ , $\eta_{\text{PL}}$, $\eta_{\text{abs}}$, $\eta_{\text{DC}}$ and $\eta_{\text{MPE}}$ were fixed. Experiments were carried out to determine the optimum PV to LSC ratio and PV cell placement in order to optimize $A_{\text{PV}}/A_{\text{panel}}$ and $A_{\text{LSC}}/A_{\text{panel}}$. Waveguide thickness and edge properties were also varied to optimize $\eta_{\text{WG}}$ to effect maximum photon collection for the size of the PV cells used.

## 2. Experimental methods

### 2.1. Construction of LSC windows

Photovoltaic cells (Sun Power, unless otherwise noted), 1 cm × 12.5 cm and 2 cm × 12.5 cm in dimension, were optically attached (Sylgard 184 silicone elastomer, unless otherwise noted) to a clear, rigid, acrylic panel. Flexible acrylic sheets, 500 μm thick embedded with Lumogen Red 305 (LR305) dye, were fused (Weld-On 4SC solvent) to clear spaces on the acrylic panels surrounding the PV cells (Fig. 1II). The thin LR305 embedded sheets acts as the absorbing layer for incident photons while the clear acrylic serves as a waveguide for concentrating those photons. PV cells and luminescent material were arranged in various configurations to study how cell placement affects power output and gain in the LSC window (or panel, words used interchangeably).

### 2.2. Optical measurements

Steady-state absorption spectra were taken using an N&K UV–vis spectrometer. Steady-state photoluminescence (PL) spectra were measured with an LS-45 Perkin Elmer spectrometer.

To measure photon reabsorption of the LSC material, a sample of the luminescent dye embedded in PMMA was attached to an acrylic waveguide. The edge was inserted into an integrating sphere (Labsphere), which was attached to a spectrometer (Ocean Optics). The spectrum of emitted light from the edge was measured for increasing distances between the edge and the light source (AM1.5 light simulator).

Quantum yields of solid films were measured using an integrating sphere (Horiba Jobin Yvon) attached to a Fluorolog-3

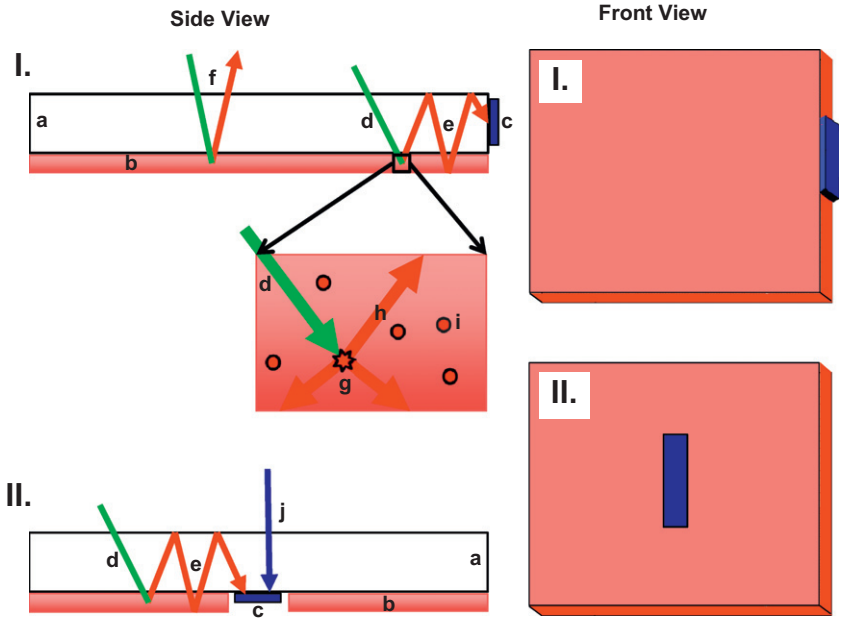


**Fig. 1.** Schematic of conventional LSC design with side-mounted PV cells (I) with a magnified view of dye molecules embedded in the flexible acrylic sheet (inset); innovative LSC design with front-facing PV cells (II). a, acrylic panel; b, luminescent sheet; c, PV cell; d, incident photon absorbed by luminescent dye; e, photon emitted by luminescent dye, wave-guided and absorbed by PV cell; f, incident photon absorbed by luminescent dye and re-emitted at angle within escape cone; g, dye molecule excited by photon, light is downshifted and re-emitted isotropically; h, downshifted photon is re-emitted into the waveguide; i, dye molecule; and j, direct sunlight absorbed by front-facing PV cell.

spectrometer (Horiba). Films were mounted in a solid sample holder at 22.5° incidence to the incoming 573 nm excitation. Excitation and luminescence measurements were collected at a 90° angle from incidence through a 1 nm slit. Dark spectra were subtracted from sample spectra, and then intensity values at each wavelength were corrected based on prior measurements of a calibrated light source. The integrated areas of the excitation peaks (568–580 nm) relative to those of the corresponding blank samples were used to determine absorbed photon counts. The emission photon counts, i.e. the integrated areas of the emission peaks (578–780 nm) were divided by the absorbed photon counts to arrive at the quantum yield.

### 2.3. Electrical measurements

The short circuit current Isc, open circuit voltage $V_{oc}$, and resulting output power were measured using a Fluke 26 III multimeter. The measurements were taken outdoors lying flat unless otherwise noted. To obtain a correlation between the area of luminescent material surrounding the PV cell and the gain, masking experiments were performed. By placing a PV cell in the middle of an acrylic panel (45.7 cm × 45.7 cm) and covering the LSC panel with a mask template, we sequentially exposed increasing amounts of surrounding luminescent area to sunlight, recording the current and voltage values. The resulting power was compared against the power of a reference cell and the power of the sun (using a pyranometer, Apogee MP-200) to obtain the gain and efficiency, respectively. The reference reading used was obtained by masking off all luminescent material leaving only the PV cell under clear acrylic exposed. Both 1 cm wide and 2 cm wide cells were tested using the same set up.

## 3. Results and discussion

### 3.1. Optical properties of the luminescent absorber

Lumogen Red 305 (LR305) was chosen as the LSC luminescent material due to its high quantum yield and stability in air [28]. Absorption (green curve) and PL emission (red curve) for LR305 embedded in PMMA are shown in Fig. 2A. Clear PMMA was used as a base line scan for absorption spectroscopy. LR305 absorbs strongly below 400 nm and in the 500–600 nm range. Between 400 and 500 nm, absorption drops to an average value of 61% with a peak at 573 nm. The extinction coefficient at 573 nm was calculated to be $4.0 \times 10^4$. For 437 nm excitation, the PL emission spectrum peaks at 611 nm and has a shoulder around 650 nm. Photon reabsorption in the LSC shifts the emission peak toward the 650 nm shoulder gradually reducing the overlap between absorption and emission spectra, as shown in Fig. 2B. The LR305 was embedded into a flexible acrylic sheet of 500 μm thickness in which it has a quantum yield of 85% ( ± 3%).

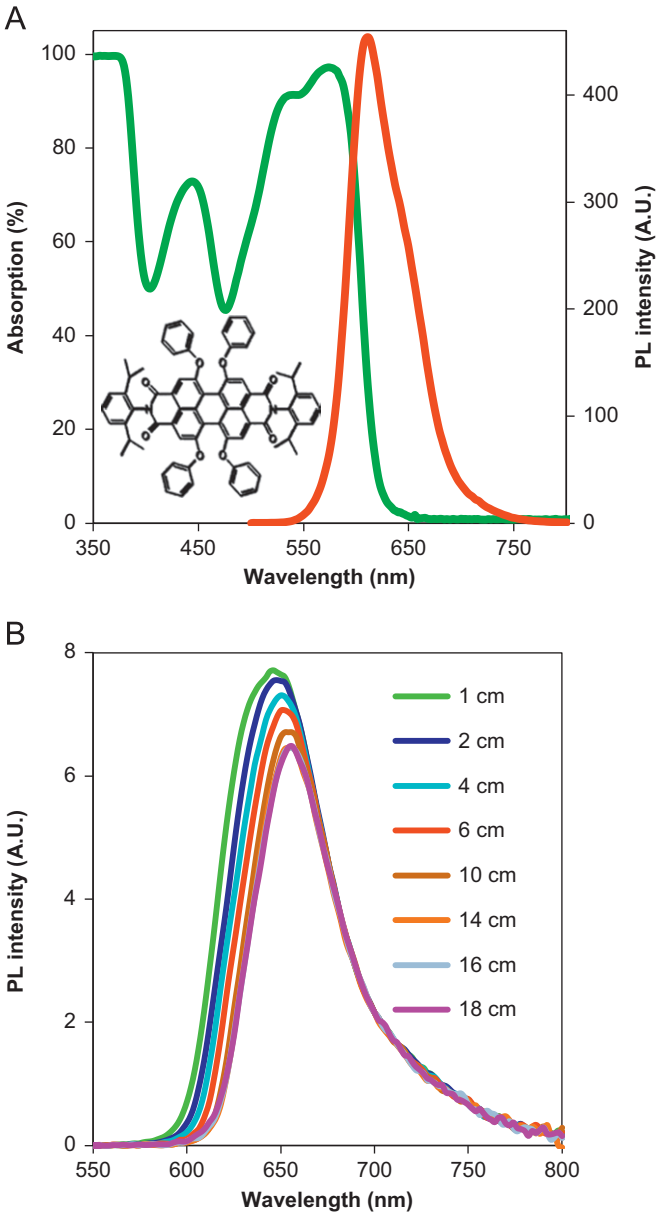


**Fig. 2.** Steady state absorption (green curve) and photoluminescence emission (red curve) spectra for LR305 (top). Photoluminescence emission spectra of LR305 embedded in an acrylic sheet for increasing distances between excitation and detection (bottom). Inset, molecular structure of LR305. (For interpretation of the references to color in this figure caption, the reader is referred to the web version of this article.)

### 3.2. Optimization of LSC window parameters: acrylic thickness, edge treatment

Several waveguide parameters can be adjusted to increase the amount of light collected by an attached PV cell, two of which are the waveguide thickness and its edge surface properties. Thicker waveguides reduce reabsorption losses but increase the likelihood of photons passing over the PV cell uncollected. The effect is reversed for thinner waveguides. In addition, a waveguide that is too thin will cause the majority of trapped photons to be directed to the edges of the PV cell, leaving the middle unenhanced by the LSC. Hence waveguide thickness and PV cell size must be properly matched. Acrylic sheet waveguides, 30.5 cm × 30.5 cm, of 4 different thicknesses, 1/16" (0.159 cm), 1/8" (0.318 cm), 3/16" (0.476 cm), and 1/4" (0.635 cm), were used to construct LSC panels and the power output of a 1 cm wide PV cell on each window was tested. For this cell dimension, the 3/16" (0.476 cm) thick acrylic was found to provide the highest power output, and all designs thereafter were based on this thickness.

Next the effect of the waveguide edge on performance was investigated. With rough untreated edges, the probability of trapped light refracting out of the waveguide at the edge is high. Treating the edge to increase reflectivity so that trapped light will not escape at the edges of the panel was used to increase the amount of light collected by the PV cell. Ideally, a surface that is 100% reflective would be engineered to completely remove this mode of loss.

To test the impact of the edge treatment, two 22.8 cm × 22.8 cm LSC windows were constructed. Each window had one

**Table 1**
Power output for various acrylic edge treatments.

| Edge coating | Power (W) | |
|---|---|---|
| | Rough | Fire polished |
| Reflective | 0.470 | 0.489 |
| None | 0.423 | 0.441 |
| Black | 0.378 | 0.378 |

1 cm × 12.5 cm PV cell placed in the center. One had the edges fire-polished to create a smooth vertical wall and the other was left untreated. The surface was further modified in each experiment by coating the edges with black tape, silver-colored reflective tape or left unmodified. The power output was measured for each case and is shown in Table 1. With black coating, both panels had the same power, as expected since all waveguided light reaching the edge would be absorbed. This was used as a check to ensure that both panels had the same starting conditions. The fire-polished panel showed an increase in power of 4% over the rough edge panel, both with and without reflective coating. Fire-polish treatment was again applied to a more complex Tic-Tac-Toe window (described below) but showed no significant improvement. This treatment being both time-consuming and costly was discontinued. The addition of a reflective coating increased power output by 11% compared to uncoated edges in both the rough and fire-polished panels. On the masking panel (described below), the addition of reflective coating resulted in a 12% increase in power. All subsequent demos had the edge treated with reflective coating.

### 3.3. *Optimization of LSC window parameters: design projections, cell width*

The next parameter investigated was the gain as a function of the LSC area exposed around the PV cell. A larger LSC area collects more light and concentrates it onto the PV cell, thus increasing its gain. At the same time, a larger proportion of that waveguided light travels a longer distance before reaching the PV cell, incurring losses along the way and dropping the increase in gain per area. Masking results for 2 cm PV cell, as seen in Fig. 3, show that the gain per area LSC plummets significantly from 2 to 6 cm of LSC exposed around the cell and flattens out as photon re-absorption decreases resulting from the increased redshift of emission that occurs with distance in the waveguide (Fig. 2B). It was also observed that LSC material placed along the long edge of the PV cell (Fig. 4B) contributes a greater gain per area than LSC along the narrow edge of the PV cell (Fig. 4A). This can be seen in Fig. 4, which shows the gain with two different shaped masks. The first mask is rectangular, the same shape as the cell, as to expose area equally around the cell. The second mask is square, the same shape as the panel so that the dimension of the mask would stay constant until the whole of the panel was exposed. As seen in Fig. 4 (inset), a dye molecule emitting photons isotropically located at the long-edge of the PV cell will emit photons to be absorbed by the cell over a larger angle than one located the same distance from the short edge of the cell. Therefore, LSC adjacent to the long-edge emits light that has a higher probability of being waveguided to the PV cell than LSC along the short-edge, thus provides a greater contribution to the gain.

From Fig. 4, there is a discernible difference in the gain obtained from masking and from LSC panels cut to the same dimension as the mask (labeled as cut to size). The masking experiments consistently underestimate the level of actual gain. This is largely due to additional losses experienced by waveguided light traveling underneath the mask to the panel edges

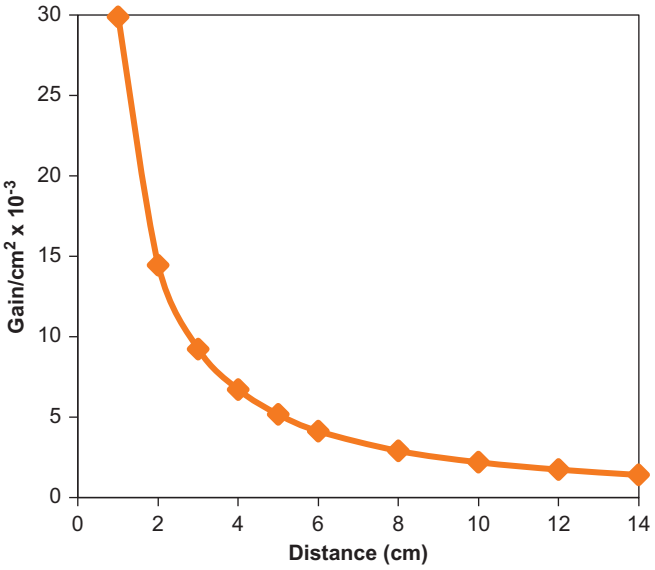


**Fig. 3.** Gain per area for increasing distances of exposed LSC material to PV cell.

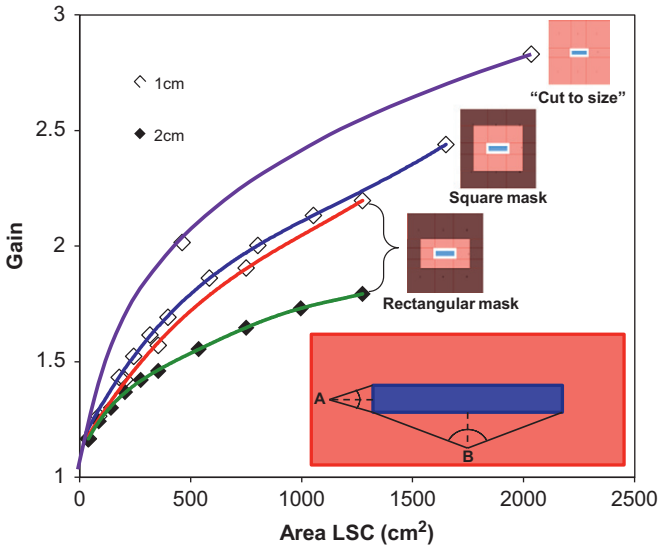


**Fig. 4.** Gain as a function of LSC area surrounding a PV cell in masking experiments and "cut-to-size" windows. Inset, schematic illustrating that LSC exposed on the long-edge of the PV cell contributes greater gain than the LSC on the short-edge of the cell.

before being reflected back, instead of doing so at the mask edge as a "cut to size" panel would. As mentioned throughout this paper, longer distances spent in the panel increases the probability of photon of re-absorption or scattering. This discrepancy between masked and "cut-to-size" is factored into our measured masking data accordingly for our design projections in Fig. 5, labeled as "corrected".

Plotting the gain against the percentage area of LSC coverage, we were able to make projections of the area ratio needed to produce panels of a desired efficiency or gain. Projections were calculated assuming the PV cells had 18% efficiency. For high gain, we estimated from Fig. 5 that a 98–98.5% LSC coverage would yield a gain of 2 ×. Similarly for high power efficiency, approximately 72–77% LSC coverage would produce a window power conversion efficiency of 6%. Based on these projections, demos were constructed to attain each individual goal. There exists a tradeoff between power efficiency and gain. To achieve a high gain requires a much higher ratio of LSC, which lowers the power

conversion efficiency of the LSC window. The converse is also true for the high efficiency panel. To attain both targets simultaneously necessitates improving the gain beyond ratio adjustments. This led us to explore further the effect of cell placement on the gain and power output. Several different designs were constructed and are discussed in Section 3.4.

In the masking experiments, the 2 cm PV cell had much lower gain per LSC area exposed compared to the 1 cm PV cell on the same setup, as seen in Fig. 4. One possible reason is that the ratio of LSC area to PV cell area is halved for the 2 cm cell. Normalizing the plot in Fig. 4 to percentage LSC area, Fig. 5, yielded a much better correlation between the two curves, but the question still arises, which width of cell, 1 cm or 2 cm, would lead to the optimal design? Two 1 cm cells would compose a design with a greater amount of LSC directly adjacent to the cells, allowing photons to be collected after traveling a shorter distance in the LSC. One 2 cm cell though yields a more compact design allowing more energy conversion. To satisfy this query, three new panels were constructed for 1 cm and 2 cm cells keeping the PV to LSC ratio the same as shown in Fig. 6. An 18 cm × 18 cm panel was constructed with one 1 cm × 12.5 cm cell in the center. Two 25.3 cm × 25.3 cm panels were constructed, one with one 2 cm × 12.5 cm cell in the center, and one with two equally spaced 1 cm × 12.5 cm cells.

The output power shown in Table 2 was normalized between the cells since the width of the 1 cm cell (0.96 cm) was not in fact half that of the 2 cm cell (1.8 cm), and both dimension of cells had different fill factors. After normalizing, the power output and gain of the single 1 cm and 2 cm panels (Fig. 6A and C) were found to be similar, indicating little difference in performance. Of greater interest is the better gain and normalized power seen in the two 1 cm panel (Fig. 6B) compared to the 2 cm panel, as a result of a change in cell placement. Redistributing the PV area permits wave-guided photons a shorter traveling distance before being collected by the cell. However, cutting the PV cells to size introduces defects into the crystal structure, which act as current shunting pathways that lower the fill factor and output current of the cell. Hence, cutting the cells into smaller pieces is only justified if this loss is more than compensated by an increase in gain through optimized cell layout and panel dimensions. The comparison of 1 cm and 2 cm cells was further explored by constructing more complex windows of identical design using both types of cells, as explained in the following section and shown in Fig. 8.

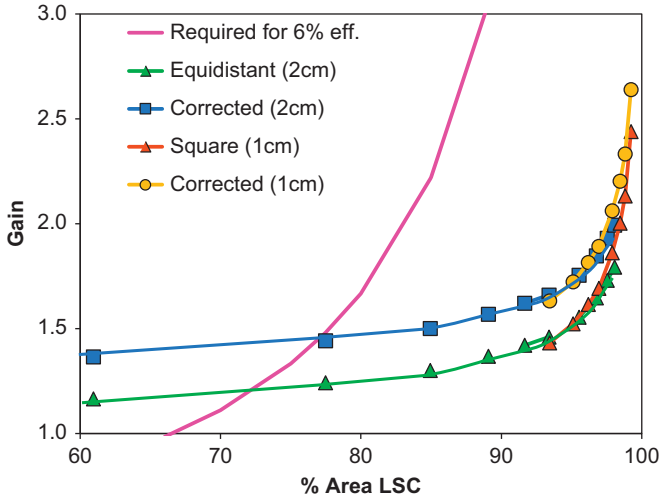


**Fig. 5.** Projected gain and window efficiency as a function of % LSC area. Projections calculated for 18% efficient PV cells.

### 3.4. LSC window demos

In analyzing the efficiency and gain in the different designs, measurements were taken under three conditions, which yielded varied results. Fig. 7B which depicts the three ways measurements were taken: with a flash tester (Sinton Instruments), outside with the window lying flat, and outside with the window tilted normal to the sunrays; Table 3 exemplifies the differences in measurements for the High Power Efficiency window, described below.

Light incident on the LSC at an angle greater than 90° increases the path length of light in the LSC thereby increasing the absorption by the dye and hence the gain. Additionally, the PV cell's efficiency is dependent on the angle of incidence. Best efficiencies are obtained with light at normal incidence and deteriorate with increasing angles as seen in Table 3. Taken together, angled light on the LSC window (resulting from taking measurements with the panel laying flat) favors higher gain due to a slightly greater contribution from the LSC and significantly poorer power contribution from the PV cell.

Flash testing involves illuminating the panel with a short burst of simulated sunlight. This prevents the PV cells from heating up

**Table 2**
Power output and gain for cell width demos in Fig. 6.

| Panel | Cell area ($cm^2$) | Power (W)[a] | Normalized power (W)[b] | Gain |
|---|---|---|---|---|
| One **1 cm** cell | 12 | 0.360 | 0.674 | 1.9 |
| Two **1 cm** cells | 24 | 0.777 | 0.728 | 2.0 |
| One **2 cm** cell | 22.5 | 0.699 | 0.699 | 1.8 |

[a] 1 cm fill factor is 0.679, 2 cm fill factor is 0.723
[b] Normalized by cell area

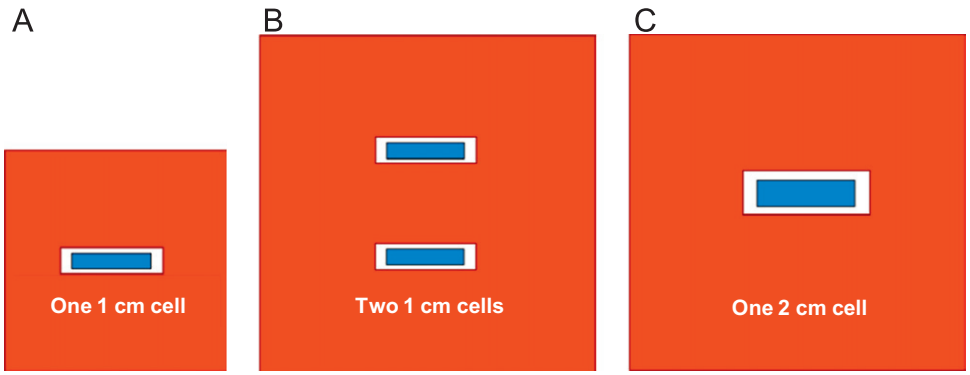


**Fig. 6.** Cell width demos. A, panel with one 1 cm wide PV cell; B, panel with two 1 cm wide PV cells; and C, panel with one 2 cm wide PV cell.

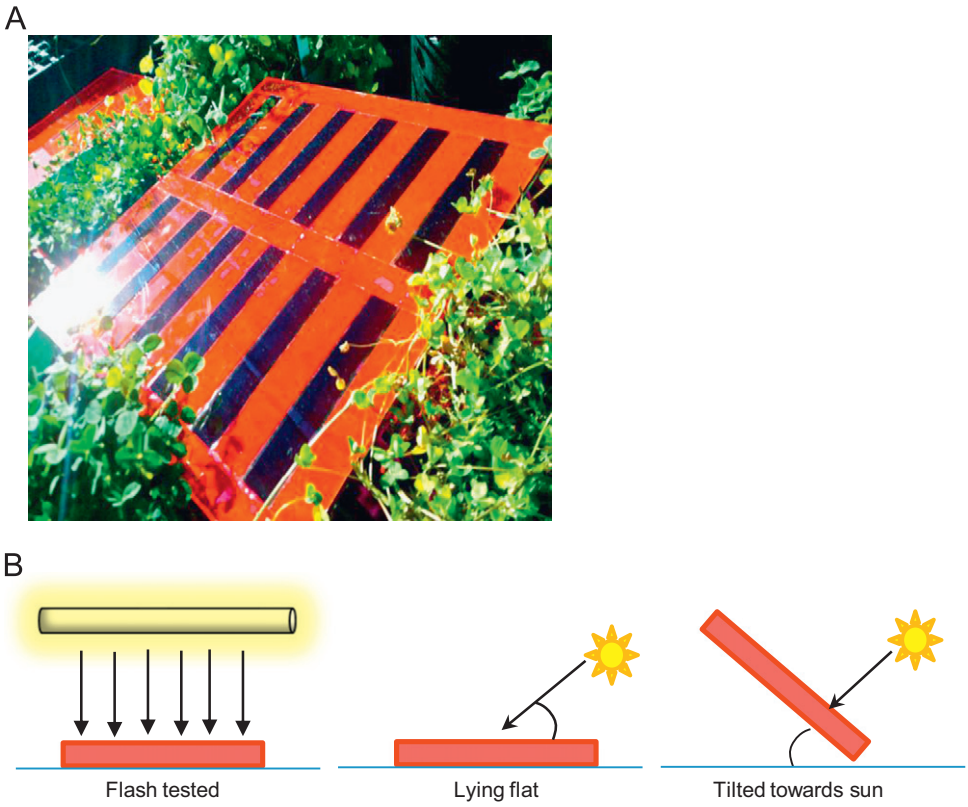


**Fig. 7.** Case study: testing methods on high power efficiency window. A, High power efficiency window; B, different testing methods: flash tester; outside with demo lying flat; and outside with demo tilted towards the sun.

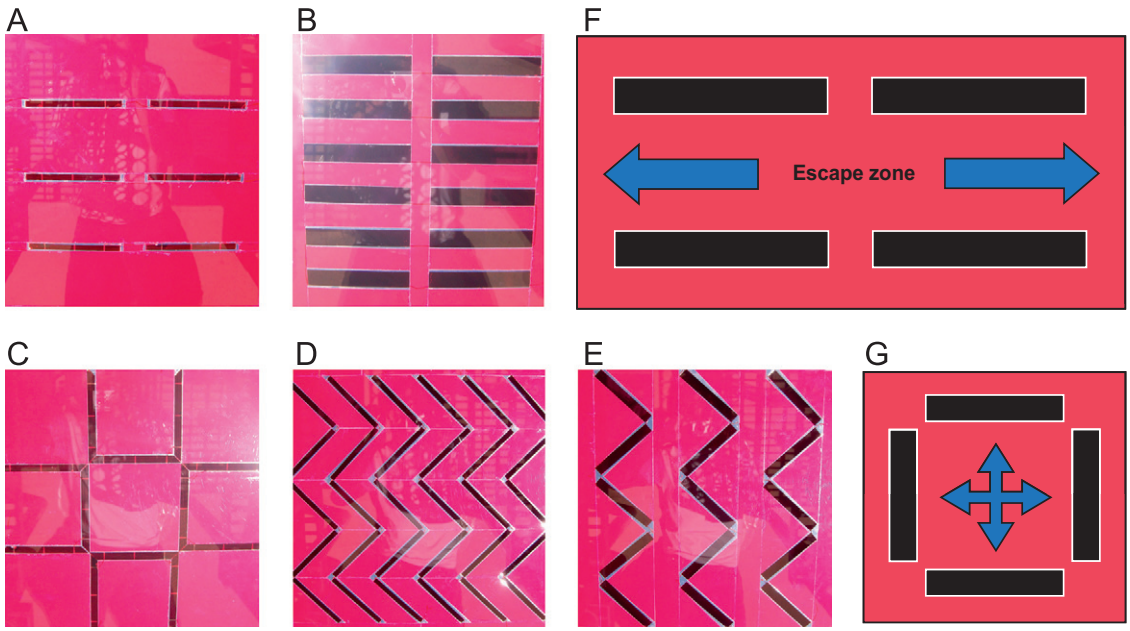


**Fig. 8.** Design of LSC windows. A, high gain; B, high power efficiency; C, Tic-Tac-Toe; D, 1 cm Zig-Zag; E, 2 cm Zig-Zag. Sample layouts showing potential escape zones (F) and superior light trapping (G).

**Table 3**
Summary of variations in gain and efficiency for different testing methods.

| Method | Gain | Reference cell efficiency (%) | Panel efficiency (%) |
|---|---|---|---|
| Flash | 1.2 | 19.8 | 6.8 |
| Flat | 1.4 | 15.5 | 6.2 |
| Tilted | 1.2 | 18.4 | 6.6 |

and thus yields a higher measured $V_{oc}$ compared to outdoor measurements, and hence a higher cell efficiency. As seen in Table 3, the gain of the panel when flash tested was approximately the same as the tilted measurements but with higher efficiencies recorded.

Gain for the panels measured outdoors was somewhat variable and depended on the month and time of the day measurements

**Table 4**
LSC window performance summary. Gain and panel efficiency measured with flash tester.

| Demo | Panel area ($cm^2$) | LSC coverage % | Panel efficiency % | Gain |
|---|---|---|---|---|
| High power efficiency | 1011 | 69 | 6.8 | 1.2 |
| Zig-Zag 1 cm | 2581 | 85 | 3.7 | 1.6 |
| Zig-Zag 2 cm | 2581 | 86 | 3.8 | 1.6 |
| Tic-Tac-Toe[a] | 2088 | 90 | — | 1.6 |
| High gain[a] | 2088 | 95 | — | 1.8 |

[a] Efficiencies are not comparable to other demos because of difference in cell type

**Table 5**
Cost per watt for all demos. The right-most column was calculated with \$1.90/W (Sun power cells) converted to cost/$m^2$ for 20% efficient cells.

| Demo | LSC coverage | \$/W[b] |
|---|---|---|
| 18% efficiency PV cell | 0% | \$2.11 |
| High power efficiency | 69% | \$1.77 |
| Zig-Zag 1 cm | 85% | \$1.64 |
| Zig-Zag 2 cm | 86% | \$1.52 |
| Tic-Tac-Toe[a] | 90% | \$1.65 |
| High gain[a] | 95% | \$2.29 |

[a] Power calculated with 0.7 fill factor in order to compare \$/W with demos using Sun power PV cells.
[b] Calculated based on Sun power PV cost of \$380/$m^2$ and LSC material cost of \$10/$m^2$

taken. This was largely due to the changes in the angle of the sun. To the best of our abilities, we took outdoor measurements within the same 2–3 h time slot each day but could not correct for monthly variations in the sun's angle or variation of the sun's intensity. As such, an objective comparison between panels can only be carried out with the flash test data as reported in Table 4. Since angled light produces a greater contribution from the luminescent dye, panels with high LSC coverage would exhibit significantly smaller gain with the flash tester compared to outdoors.

A high gain window was built to have a gain of 2 × with 95% LSC coverage on a 45.7 cm × 45.7 cm panel. Six 1 cm × 15.5 cm PV cells (Evergreen Solar) were arranged in three rows of two, equidistant from each other and the panel edges, as shown in Fig. 8A. Less LSC coverage was used than projected due to expected improvements in performance from cell placement and additional reflected light from the closer proximity of the window edges to the cells.

The window was tested outdoors lying flat and attained a gain of 2.2 ×. Adding a white reflective background returned a portion of the transmitted and escaped light to the window and raised gain further to 2.4 ×. Flash testing with light entering normal to the panel surface gave a lower gain of 1.8 ×. Power efficiency cannot be accurately compared to other window designs because a different PV cell type was used.

A high power efficiency demo, targeted to have a power conversion efficiency of 6%, was built with 69% LSC coverage on a 31.8 cm × 31.8 cm panel. Twelve 2 cm × 12.5 cm PV cells were arranged in six rows of two, equidistant from each other and the edges, as shown in Fig. 8B. Data taken with the panel lying flat attained a power conversion efficiency of 6.2%, with a gain approaching 1.4 ×. A maximum panel efficiency of 6.8% was obtained with flash testing. Results are summarized in Table 3.

In the above two designs, we see many large zones that light can potentially travel and reflect multiple times without ever hitting a PV cell as illustrated in Fig. 8F. While photons may eventually scatter in a favorable direction, the likelihood of the photon being lost increases with distance traveled after the initial absorption event. A better design reduces these escape zones and increases the amount of light collected as shown in Fig. 8G.

To find a balance between gain and panel efficiency, two demos with a "Tic-Tac-Toe" pattern were built with 90% LSC coverage on 45.7 cm × 45.7 cm panels. Twelve trapezoidal 15 cm × 12.5 cm × 1.2 cm PV cells (Evergreen Solar) were arranged in a Tic-Tac-Toe formation as shown in Fig. 8C. One Tic-Tac-Toe window was created on an acrylic panel with fire-polished edges and one Tic-Tac-Toe window was created on an acrylic panel with rough (untreated) edges. Reflective coating was applied to the edges of both demos.

This design was projected to have a gain of 1.6 × based on the masking experiments but attained a factor of 1.8 × outdoors. The design was chosen to better capture light radiating isotropically in the LSC material. The panel power efficiency cannot be compared to the other demos due to a difference in PV cell type used. No difference was observed between the panel with fire-polished edges versus the one with rough edges. Fire-polishing acrylic edges appear to have no effect on power output and gain in this design.

To further improve light trapping, a Zig-Zag pattern was constructed next. Two Zig-Zag demos with different cell widths were built on 50.8 cm × 50.8 cm acrylic panels, as shown in Fig. 8D and E, and were designed to have the same LSC coverage. One panel was built with 15–2 cm PV cells and the other was built with 30–1 cm PV cells. Inaccuracy in dicing resulted in actual cell widths of 1.8 cm and 0.96 cm, respectively, giving both panels slightly different cell coverage than intended.

The 1 cm and 2 cm Zig-Zag demos had a LSC coverage of 85% and 86%, respectively. The demos attained gains of 1.4 × and 1.5 × when tested outdoors, against a projected gain of 1.5 ×. Construction of the Zig-Zag design was much more complicated than any of the previous panels, resulting in many defects, especially in the seams where LSC pieces were joined. The additional scattering could have adversely affected the panel performance. This drawback might be overcome by laminating the LSC directly over the cells in future iterations. Panel conversion efficiency was calculated using power output measurements taken with a flash tester. The 1 cm Zig-Zag demo reached a panel conversion efficiency of 3.7% and the 2 cm Zig-Zag demo reached 3.8% efficiency.

Table 4 provides a summary of the dimensions and performance of all windows/panels constructed.

### 3.5. Cost per watt optimization

The ultimate objective of this project is to reduce the added cost per watt of solar electricity by incorporating solar cells into a window. In that respect, pushing for high efficiency or high gain does not result in the lowest cost as seen in Table 5. The tradeoff between gain and high energy-conversion efficiency is non-linear and a design with the best compromise of these design factors, which in our case is the 2 cm Zig-Zag panel, achieves the lowest cost. Further improvements can be expected by further increasing the gain while maintaining the same coverage. The ongoing goal of removing as many loss mechanisms as possible is in future works.

## 4. Conclusion

Front facing PV cells allow us flexibility in designing LSC windows with varied cell coverage and cell placement. The relationship of the gain as a function of LSC exposed in the masking experiments shows a non-linear relationship between gain per unit area and panel efficiency. From the results,

we obtained estimates on the minimum coverage needed for each design and noted that area on the short edges of the cell can be sacrificed with minimal impact to performance. These considerations were later incorporated into our cell placement strategies. Cost analysis indicates, contrary to initial expectations, pursuing a high gain at the expense of efficiency resulted in an overall higher cost per watt, even though the LSC material itself was inexpensive. Due to the non-linear tradeoff between gain and efficiency, our demos show that a cell coverage of 14% yielded the lowest cost. Analysis of existing windows shows many light loss mechanisms that can still be addressed and future work will be geared towards increasing the absorption spectrum of the LSC and reducing re-absorption losses.

## Acknowledgments

This work was supported by the U.S. Department of Energy Grant No. DE-EE0003455 and by the University of California Discovery Grant No. 192864. Portions of this work were performed at the Molecular Foundry and were supported by the Office of Science, Office of Basic Energy Sciences, of the U.S. Department of Energy under Contract No. DE-AC02-05CH11231. We would also like to thank Jeremy Olson, Nathan Green, Shila Alavi, and Glenn Alers at APV Research as well as Dave Thayer in the Wood Shop at UCSC.

## References

[1] P. Lorenz, D. Pinner, T. Seitz, The economics of solar power, The McKinsey Q (2008) 1–10.
[2] V. Fthenakis, J.E. Mason, K. Zweibel, The technical, geographical, and economic feasibility for solar energy to supply the energy needs of the US, Energy Policy 37 (2009) 387–399.
[3] B.S. Richards, Enhancing the performance of silicon solar cells via the application of passive luminescence conversion layers, Solar Energy Materials and Solar Cells 90 (2006) 2329–2337.
[4] L.H. Slooff, E.E. Bende, A.R. Burgers, T. Budel, M. Pravettoni, R.P. Kenny, E.D. Dunlop, A. Büchtemann, A luminescent solar concentrator with 7.1% power conversion efficiency, Physica status solidi 2 (2008) 257–259.
[5] L.H. Slooff, R. Kinderman, A.R. Burgers, A. Büchtemann, R. Danz, T.B. Meyer, A.J. Chatten, D. Farrell, K.W.J. Barnham, J.A.M. van Roosmalen, The luminescent concentrator illuminated, Proceedings of SPIE 6197 (2006) 61970 K.
[6] W.G.J.H.M. van Sark, K.W.J. Barnham, L.H. Slooff, A.J. Chatten, A. Büchtemann, A. Meyer, S.J. McCormack, R. Koole, D.J. Farrell, R. Bose, E.E. Bende, A.R. Burgers, T. Bundel, J. Quilitz, M. Kennedy, T. Meyer, C. de Mello Donega, A. MeijerinkD. Vanmaekelbergh, Luminescent solar concentrators—a review of recent results, Optics Express 16 (2008) 21773–21792.
[7] R. Koeppea, N.S. Sariciftci, Enhancing photon harvesting in organic solar cells with luminescent concentrators, Applied Physics Letters 90 (2007) 181126-1–181126-3.
[8] R. Koeppea, O. Bossart, G. Calzaferri, N.S. Sariciftci, Advanced photon-harvesting concepts for low-energy gap organic solar cells, Solar Energy Materials and Solar Cells 91 (2007) 986–995.
[9] M.J. Currie, J.K. Mapel, T.D. Heidel, S. Goffri, M.A. Baldo, High-efficiency organic solar concentrators for photovoltaics, Science 321 (2008) 226–228.
[10] G.V. Shcherbatyuk, R.H. Inman, C. Wang, R. Winston, S. Ghosh, Viability of using near infrared PbS quantum dots as active materials in luminescent solar concentrators, Applied Physics Letters 96 (2010) 191901-1–191901-3.
[11] M.G. Debije, P.P.C. Verbunt, Solar Concentrators: thirty years of luminescent solar concentrator research: solar energy for the built environment, Advanced Energy Materials 2 (2012) 1–168.
[12] E. Klampaftis, D. Ross, K.R. McIntosh, B.S. Richards, Enhancing the performance of solar cells via luminescent down-shifting of the incident spectrum: a review, Solar Energy Materials and Solar Cells 93 (2009) 1182–1194.
[13] C. Strumpel, M. McCann, G. Beaucarne, V. Arkhipov, A. Slaoui, V. Svrcek, C. del Canizo, I. Tobias, Modifying the solar spectrum to enhance silicon solar cell efficiency—An overview of available materials, Solar Energy Materials and Solar Cells 91 (2007) 238–249.
[14] E. Klampaftis, B.S. Richards, Improvement in multi-crystalline silicon solar cell efficiency via addition of luminescent material to EVA encapsulation layer, Progress in Photovoltaics 19 (2011) 345–351.
[15] A.M. Herman, Luminescent solar concentrators—a review, Solar Energy 4 (1982) 323–329.
[16] W.H. Weber, J. Lambe, Luminescent greenhouse collector for solar radiation, Applied Optics 15 (1976) 2299–2300.
[17] C.F. Rapp, N.L. Boling, Luminescent solar concentrator, IEEE Photovoltaic Specialists Conference (1978) 690–693.
[18] A. Goetzberger, W. Greubel, Solar energy conversion with fluorescent collectors, Applied Physics 14 (1977) 123–139.
[19] B. Norton, P.C. Eames, T.K. Mallick, M. Huang, S.J. McCormack, J.D. Mondol, Y.G. Yohanis, Enhancing the performance of building integrated photovoltaics, Solar Energy 85 (2011) 1629–1664.
[20] D. Chemisana, Building integrated concentrating photovoltaics: a review, Renewable & Sustainable Energy Reviews 15 (2011) 603–611.
[21] B. Rezaie, E. Esmailzadeh, I. Dincer, Renewable energy options for buildings: case studies, Energy and Buildings 43 (2011) 56–65.
[22] B.C. Rowan, L.R. Wilson, B.S. Richards, Advanced material concepts for luminescent solar concentrators, IEEE Journal of Selected Topics in Quantum. Electronics 14 (2008) 1312–1322.
[23] R. Reisfeld, Prospects of sol-gel technology towards luminescent materials, Optical Materials 16 (2001) 1–7.
[24] S.J. Gallagher, B. Norton, P.C. Eames, Quantum dot solar concentrators: electrical conversion efficiencies and comparative concentrating factors of fabricated devices, Solar Energy 81 (2007) 813–821.
[25] J. Bomm, A. Büchtemann, A.J. Chatten, R. Bose, D.J. Farrell, N.L.A. Chan, Y. Xiao, L.H. Slooff, T. Meyer, A. Meyer, W.G.J.H.M. van Sark, R. Koole, Fabrication and full characterization of state-of-the-art quantum dot Luminescent solar concentrators, Solar Energy Materials & Solar Cells 95 (2011) 2087–2094.
[26] A.F. Mansour, On enhancing the efficiency of solar cells and extending their performance life, Polymer Testing 22 (2003) 491–495.
[27] R. Reisfeld, M. Eyal, V. Chernyak, R. Zusman, Luminescent solar concentrators based on thin films of poly-methylmethacrylate on a poly-methylmethacrylate support, Solar Energy and Materials 17 (1988) 439–455.
[28] L.R. Wilson, B.S. Richards, Measurement method for photoluminescent quantum yields of fluorescent organic dyes in polymethyl methacrylate for luminescent solar concentrators, Applied Optics 48 (2009) 212–220.